inorganics

MDPI

Article

Effect of Gold(III) on Cytotoxicity and Antimicrobial Activity of Nifuroxazide Analogs

Daniil N. Yarullin [1], Olga I. Logacheva [1], Aleksandra K. Isagulieva [2], Olga N. Sineva [3], Vera S. Sadykova [3], Maksim N. Zavalishin [1] and George A. Gamov [1,*]

[1] General Chemical Technology Department, Ivanovo State University of Chemistry and Technology, Sheremetevskii Ave. 7, 153000 Ivanovo, Russia; dn_yarullin@isuct.ru (D.N.Y.); o.logachiova@yandex.ru (O.I.L.); zavalishin00@gmail.com (M.N.Z.)
[2] Burnazyan Federal Medical Biophysical Center, Federal Medical Biological Agency, Marshal Novikov st, 23, 123098 Moscow, Russia; kia2303@yandex.ru
[3] Gause Institute of New Antibiotics, Bol'shaya Pirogovskaya st. 11/1, 119021 Moscow, Russia; olga.sineva81@yandex.ru (O.N.S.); sadykova_09@mail.ru (V.S.S.)
* Correspondence: ggamov@isuct.ru; Tel.: +7-(4932)30-73-46

Abstract

Metal ions can influence the biological activity of organic compounds, although the effects of metal addition depend on the chemical speciation of the resulting systems and their stability under biologically relevant conditions. Here, we investigated the interaction of gold(III) with nifuroxazide and eleven related hydrazones, as well as the effects of gold(III) addition on their cytotoxicity and antimicrobial activity. UV–Vis spectrophotometric titrations in dimethyl sulfoxide were analyzed using a proposed 1:2 metal-to-ligand equilibrium model, yielding conditional formation constants with log K' values of approximately 8.8–9.1 under the experimental conditions. The proposed stoichiometry and structure of the gold-containing species remain to be confirmed by independent analytical methods. The addition of tetrachloroaurate(III) generally produced no substantial change in the cytotoxicity of the hydrazones toward HCT116 and HEK293T cells, although some compound-dependent effects were observed. In agar well diffusion assays, gold(III) addition increased the growth-inhibition zones against *S. aureus* for most hydrazones at the tested concentrations. Inhibition of *P. aeruginosa* and *C. albicans* was also observed in the presence of tetrachloroaurate(III), although the contribution of the gold-containing component and the nature of its interaction with the hydrazones require further investigation. These findings demonstrate that gold(III) addition can modify the observed biological activity of nifuroxazide analogs, while further studies are required to establish the chemical speciation under biological conditions and determine whether the enhanced antimicrobial effects represent genuine pharmacological synergy.

Keywords: gold(III); nifuroxazide; hydrazone; antibiotic; cytotoxicity

Check for updates

Academic Editors: Esteban Rodríguez-Arce and Dinorah Gambino

Received: 29 September 2026
Revised: 28 October 2026
Accepted: 10 November 2026
Published: 12 November 2026

Copyright: © 2026 by the authors. Licensee MDPI, Basel, Switzerland. This article is an open access article distributed under the terms and conditions of the Creative Commons Attribution (CC BY) license.

1. Introduction

The spread of multidrug-resistant bacteria poses a growing threat to public healthcare systems across the globe, as can be illustrated by the following examples. Recently, a surge in carbapenem-resistant *Enterobacterales* was observed in New York [1,2]. Drug-resistant shigellosis is on the rise in England [3]. An outbreak of multidrug-resistant *Acinetobacter baumannii* occurred recently in the intensive care units of the national burns center of the University Hospital Zurich, Switzerland [4], and pediatric unit in China [5] (the latter

was also complicated by resistant *P. aeruginosa*-induced infection). Milton Cato Memorial Hospital in Saint Vincent and the Grenadines struggled to control a critical infection situation following reports that several patients had tested positive for multidrug-resistant strains, and an international intervention from the Pan American Health Organization was required to stabilize it [6]. If a healthcare system collapses because of war or natural disaster, the spread of multidrug-resistant strains becomes even more dangerous, as a recent report from Gaza shows [7].

The worsening global situation with regard to infectious diseases calls for a complex response that includes the development of new antimicrobial drugs. A promising way to achieve this is to enhance the effect of drugs already approved for medical use. Such enhancement may include chemical modification of the antibiotic [8,9], the use of cocrystals to improve a drug's solubility and bioavailability [10–14], or the synergistic combination of an antibiotic with another chemical that may not have antibacterial activity on its own (or shows only a limited effect) [9]. Among these additives, metal ions play an important role: when bound to a biologically active ligand, they imbue the latter with the ability to disrupt the microbial cell membrane, bind to and damage DNA, generate reactive oxygen species, inhibit enzymes, induce protein denaturation, inhibit biofilm formation, and interfere with biometal metabolism [15–17].

Among the ligands used to synthesize metal-based biologically active compounds, the most abundant are antimicrobial peptides, N-heterocyclic carbenes (NHCs), aliphatic amine-based ligands, Schiff bases, and hydrazones [18]. Schiff bases and hydrazones area particularly popular choice to be metallated in order to increase lipophilicity, which facilitates the penetration of the complex through the lipid-rich bacterial cell membrane, thereby improving intracellular accumulation and interaction with vital biomolecular targets [19]. In this regard, for the present study we have chosen a library of 11 hydrazones analogous to the well-known antibacterial drug nifuroxazide [20], together with the parent compound (see Figure 1 for the structures). The 5-nitrofuroyl moiety is common in efficient antibacterial drugs [21].

We selected the compounds from a previously investigated series of nifuroxazide analogs to assess how structural modifications affect their interaction with gold(III) and the biological effects of gold(III) addition [22]. The series includes positional isomers bearing hydroxyphenyl substituents, pyridine- and pyrazine-containing analogs, and compounds in which a nitrothiophene moiety replaces the nitrofuran moiety. This selection enables a preliminary comparison of the effects of changes in the aromatic substituent, heteroatom arrangement, and nitroheteroaromatic fragment on complex formation and biological activity. The selection was also motivated by the previously observed cytotoxicity and antimicrobial profiles of individual members of the series [22]. In particular, among these compounds, hydrazones **5** and **11** exhibit promising cytotoxicity and relatively high selectivity toward the tumor cell line HCT116 over the non-tumor HEK293T cell line, while compounds **2** and **4** show higher antibacterial potential against *S. aureus* than the parent drug nifuroxazide **1** [22].

Among the metals suitable for antibiotic modification, such elements as iridium [18], ruthenium [17,18], silver [17,18,23], gallium [17,18,24] and gold [17,18,25,26] attract special attention. It is noteworthy that nifuroxazide complexes with Pd^{2+}, Pt^{2+}, Ru^{2+} [27], Co^{2+}, Ni^{2+} [28], Mn^{2+}, VO^{2+}, and Cu^{2+} [28,29] have been synthesized, and their antimicrobial activity has been estimated. Early papers show only a slight influence of complexation on toxicity against various microbial strains [27,28], while recent results indicate an increase in activity of Mn^{2+}, VO^{2+}, and Cu^{2+} compared to free nifuroxazide.

Gold(III) complexes, aside from their toxicity related to intra- and interstrand cross-linking of DNA (analogous to cisplatin [30]), may also inhibit important enzymes involved

in mitigating oxidative stress and repairing proteins, including bacterial thioredoxin reductase [17,18,31], which leads to cell death. In our opinion, the antimicrobial potential of gold(III) coordination compounds, though well developed lately [31–33], is not yet exhausted, and thus, we decided to combine this metal with the previously studied ligands [22].

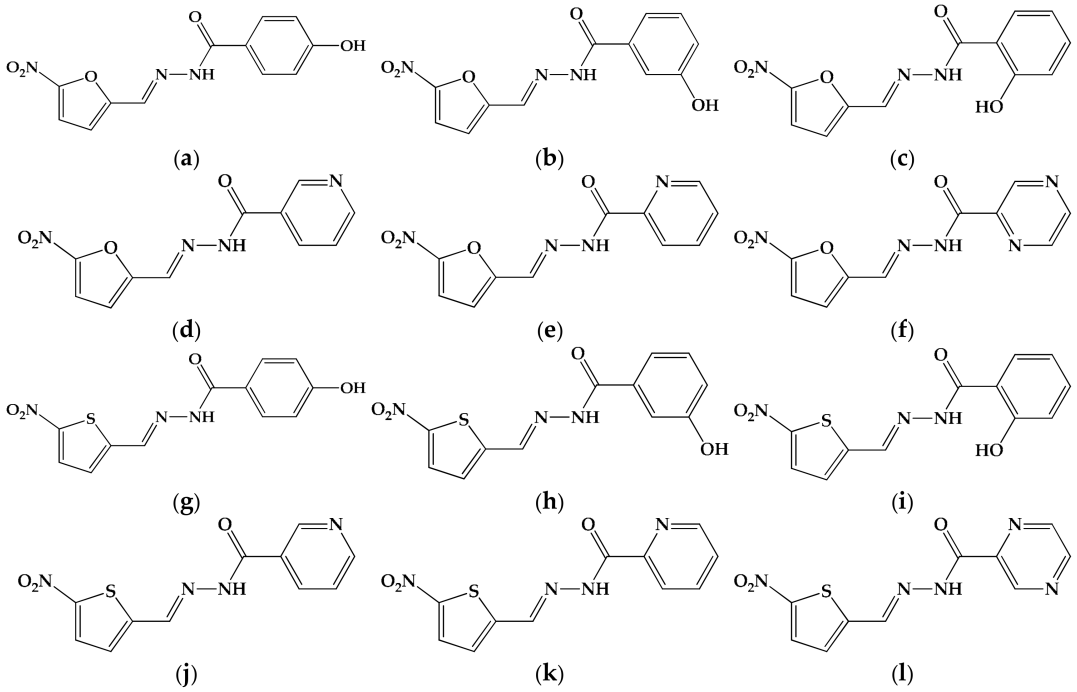


Figure 1. Structure of nifuroxazide (5-nitrofurfurylidene hydrazide of 4-hydroxybenzoic acid, **1**, (**a**)) and analogous hydrazones: 5-nitrofurfurylidene hydrazide of 3-hydroxybenzoic acid, **2** (**b**); 5-nitrofurfurylidene hydrazide of 2-hydroxybenzoic acid, **3** (**c**); 5-nitrofurfurylidene hydrazide of 3-pyridinecarboxylic acid, **4** (**d**); 5-nitrofurfurylidene hydrazide of 2-pyridinecarboxylic acid, **5** (**e**); 5-nitrofurfurylidene hydrazide of pyrazinecarboxylic acid, **6** (**f**); 5-nitrothien-2-yl hydrazide of 4-hydroxybenzoic acid, **7** (**g**); 5-nitrothien-2-yl hydrazide of 3-hydroxybenzoic acid, **8** (**h**); 5-nitrothien-2-yl hydrazide of 2-hydroxybenzoic acid, **9** (**i**); 5-nitrothien-2-yl hydrazide of 3-pyridinecarboxylic acid, **10** (**j**); 5-nitrothien-2-yl hydrazide of 2-pyridinecarboxylic acid, **11** (**k**); 5-nitrothien-2-yl hydrazide of pyrazinecarboxylic acid, **12** (**l**).

Coordination to gold(III) can substantially modify the electronic properties and reactivity of organic substrates, including their electrophilic character, as demonstrated for selected Au(III)-catalyzed reactions [34]. However, the magnitude and consequences of such changes depend on the coordination environment and the electronic structure of the ligand. Whether gold(III) coordination to nifuroxazide analogs produces comparable changes in electrophilicity, and whether these changes influence antimicrobial activity (though, in general, higher electrophilicity is associated with a stronger antibacterial effect [35,36]), remain open questions.

It should be kept in mind that the mechanism of action mentioned above may also extend to eukaryotic cells. Therefore, to be used efficiently in practice, potential antibiotics based on gold(III) complexes should have relatively low cytotoxicity. At the very least, the gain in cytotoxicity should be less than that in antimicrobial activity.

It is also noteworthy that gold(III) complexes are prodrugs rather than drugs; that is, upon entering the organism, they must first be activated to exert a biological effect [37]. Such activation may include hydrolysis of the complex or ligand exchange; moreover, the metal complex may not remain intact after intravenous administration because of the action

of blood serum proteins or other compounds present in body fluids [38]. Therefore, it is necessary to study the stability of gold(III) complexes as part of a wider investigation of their biological activity.

Despite previous investigations of nifuroxazide complexes with several transition metals, the effects of gold(III) addition to nifuroxazide and its structural analogs remain insufficiently characterized. In particular, the relationship between ligand structure, the composition and stability of the gold-containing species, and the resulting biological activity has not been systematically investigated for this series of compounds. Moreover, an increase in antimicrobial activity observed upon metal addition does not necessarily indicate the formation of a stable coordination complex or a synergistic interaction, because the biological response may also arise from the intrinsic activity of the gold-containing component or changes in compound availability. Addressing these questions requires the combined assessment of solution equilibria, cytotoxicity, and antimicrobial activity, while distinguishing experimentally established observations from mechanistic hypotheses.

Thus, in the present contribution, we report on the stability of gold(III) complexes formed with nifuroxazide and its 11 analogs and elucidate how gold(III) changes the cytotoxicity and antimicrobial activity of the hydrazones studied previously [22].

2. Results

2.1. Gold(III)–Hydrazone Interactions in Solution

The interaction of gold(III) with hydrazones **1–12** was investigated via UV-Vis spectrophotometric titration in dimethyl sulfoxide (DMSO), which was selected because of the limited solubility of the ligands in water. Upon addition of an aqueous solution of tetrachloroauric acid, an increase in absorbance at 328 nm was observed for all ligands (Figure S1), indicating a change in the absorbing species in solution.

The titration data were analyzed using the equilibrium model described by Equation (1), which assumes the formation of a species with a 1:2 gold(III)-to-ligand stoichiometry:

$$[AuCl_4]^- + 2L = [AuL_2]^{3+} + 4Cl^- \quad (1)$$

The corresponding conditional equilibrium constants were calculated using KEV software, ver. 0.6.0 [39], and are summarized in Table 1. The resulting log K' values fall within the range of 8.8 to 9.1 for all twelve ligands. These values describe the data within the adopted equilibrium model and under the experimental conditions employed; they should not be interpreted as independent proof of the molecular structure or coordination geometry of the proposed species.

Table 1. Equilibrium constants (log K') of the reaction of gold(III) complex formation with hydrazones **1–12** determined in dimethyl sulfoxide at $T = 298.2$ K and $p = 0.1$ MPa without background electrolyte ($I \to 0$).

Hydrazone	1	2	3	4	5	6	7	8	9	10	11	12
log K', Equation (1)	9.0 ± 0.1 *	8.8 ± 0.1	9.0 ± 0.3	9.0 ± 0.1	8.8 ± 0.1	8.8 ± 0.3	9.0 ± 0.1	9.1 ± 0.3	8.8 ± 0.4	9.1 ± 0.1	9.1 ± 0.3	8.9 ± 0.1

* Errors given are the standard deviations calculated for three independent experiments.

Although the 1:2 model provided a better fit than the alternative 1:1 model tested for hydrazone **1** (a smaller standard deviation of the calculated equilibrium constants, better fitting quality, and lower $R_{adj.}{}^2$; Figure S3), this comparison does not exclude the possible coexistence of other gold(III) species, including partially chloride-substituted complexes. Accordingly, the formulation $[AuL_2]^{3+}$ is treated here as a proposed representation of the dominant complex species within the adopted model, rather than as an independently confirmed molecular structure.

The equilibrium constants are significantly lower than those determined for gold(III) complexes with hydrazones derived from pyridoxal or pyridoxal 5′-phosphate [40], even taking into account the different solvent (DMSO *vs.* water [40]). Moreover, the stoichiometry is different (pyridoxal- and pyridoxal 5′-phosphate-derived ligands tended to form complexes of ML composition). This is explained by the fact that nifuroxazide and its analogs are bidentate ligands capable of complexing metal ions via the carbonyl oxygen and imine nitrogen, whereas vitamin B_6-derived ligands have an additional functional group (–OH at the 3-position of the pyridinyl residue). A tentative structure of the gold(III) complexes with hydrazones **1–12** is given in Figure 2.

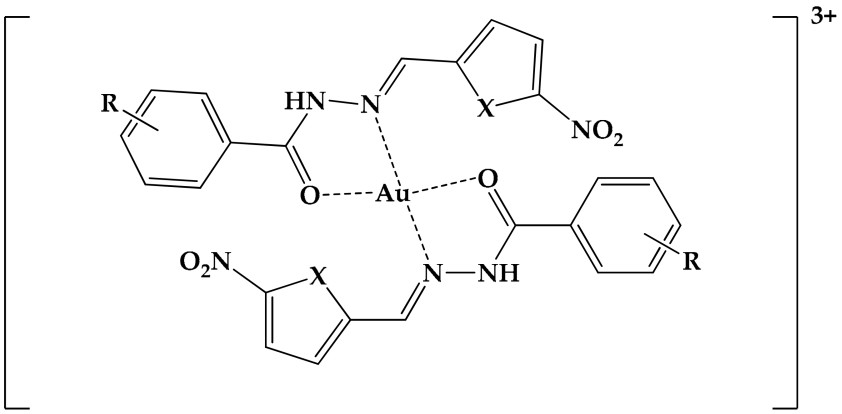


Figure 2. Proposed coordination structure of gold(III) with hydrazones **1–12**, illustrating a possible binding mode under the assumed 1:2 metal-to-ligand stoichiometry.

The similar conditional formation constants obtained for hydrazones **1–12** suggest that the structural modifications introduced across this series do not produce large differences in the spectrophotometric response described by the selected equilibrium model. However, the similarity of these constants does not independently establish the coordination sites or geometry of the gold(III)-containing species. Coordination through the carbonyl oxygen and imine nitrogen is a plausible hypothesis based on the functional groups present in the hydrazones, but alternative coordination modes and partially chloride-substituted species cannot be excluded by UV-Vis titration alone. The influence of intramolecular hydrogen bonding on complex formation likewise remains uncertain within the resolution of the present measurements.

The relatively low stability of gold(III) complexes is consistent with the data of an earlier paper [41], which provides the stability constants of Co^{2+}, Ni^{2+} and Cu^{2+} complexes with nifuroxazide (the proposed stoichiometry was ML) in alcohols. In particular, the stability constants of nickel(II) and cobalt(II) complexes do not exceed 1.6 log units, while that of the copper(II) compound reaches 3.6 log units in the least polar propan-2-ol.

The dependencies of the molar extinction coefficients on wavelength for the complexes differ only insignificantly from those of the free ligands, which was also observed for vitamin B_6-derived ligands [40] and explained by the fact that chloride substitution in the gold(III) coordination sphere by N,O-donor ligands (which have a stronger field than chloride) causes a hypsochromic shift in the UV-Vis spectrum [42].

The present study was designed to investigate the interaction of gold(III) with hydrazones **1–12** in solution and to assess the biological effects of mixing the ligands with tetrachloroaurate(III). Isolation and solid-state characterization of the proposed complexes were not undertaken. In future studies, the structure and electronic absorption spectra of gold(III) complexes with hydrazones **1–12** are to be investigated in more detail using other experimental techniques and quantum chemical methods.

2.2. Cytotoxicity of Gold(III) + Hydrazones **1–12**

The cytotoxicity of equimolar mixtures of tetrachloroaurate(III) and hydrazones **1–12** at concentrations varying from 0.2 to 50 μM was evaluated using an MTT assay against human colorectal carcinoma (HCT116) and immortalized human embryonic kidney (HEK293T) cell lines. Such concentrations, taking into account the equilibrium constants determined in this paper (Table 1), ensure complex formation in DMSO solution with a yield of ~60 mol% at the highest tested concentration of 50 μM. However, at the lowest tested concentration of 0.2 μM, the complex does not form. The results of the cytotoxicity assay, which also present the data for the free hydrazones determined previously [22], are summarized in Figure 3, and the primary dose–response data are presented in Figure S4. The effect of tetrachloroaurate(III) solution in DMSO without a ligand was also estimated: IC_{50}(HEK293T) = 34.9 μM [CI: 28.4; 42.1]; IC_{50}(HCT116) > 50 μM.

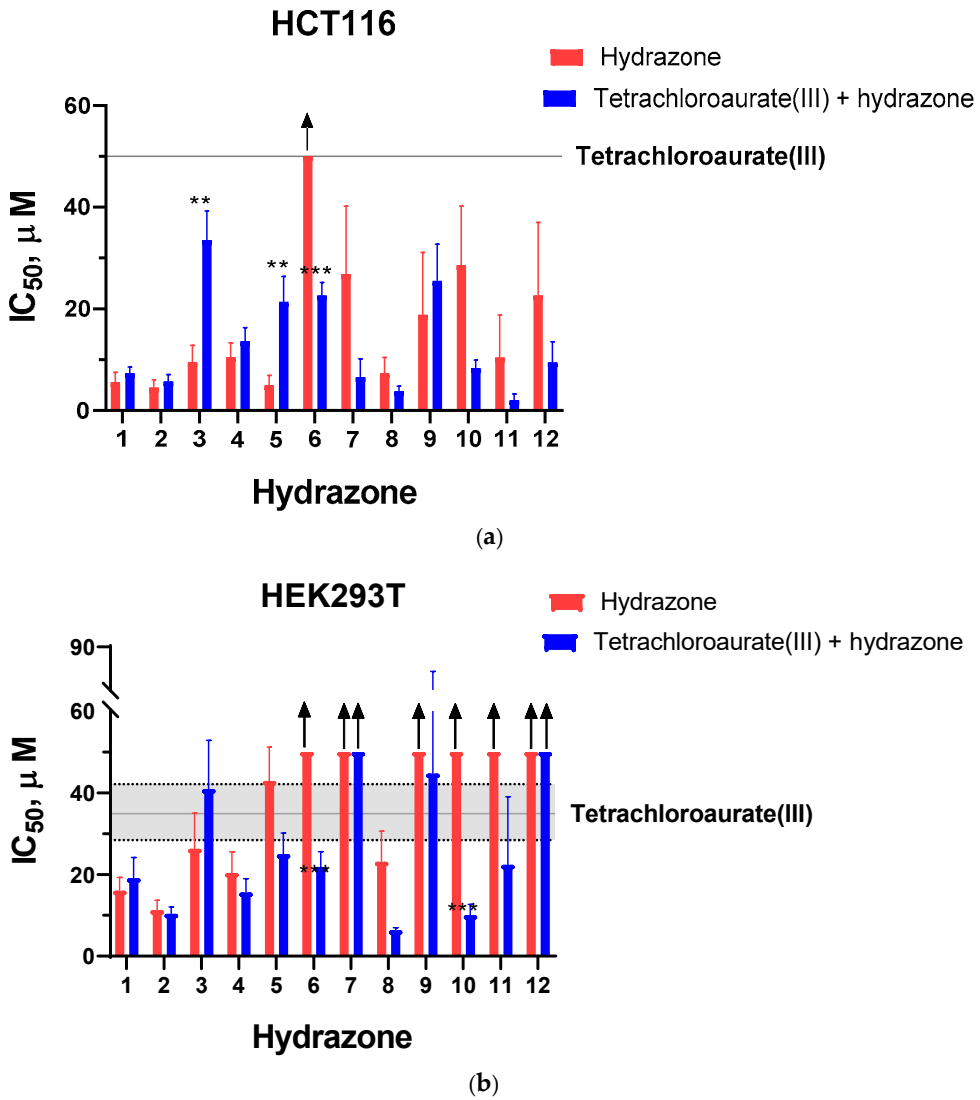


Figure 3. IC_{50} values (μM) [CI] of hydrazones **1–12** [22] and their mixtures with tetrachloroaurate(III) determined for HCT116 (**a**) and HEK293T (**b**) cell lines. Asterisks denote the statistical significance level: ** $p < 0.01$, *** $p < 0.001$. Arrows indicate compounds with IC_{50} values exceeding the tested concentration range (>50 μM). The IC_{50} of tetrachloroaurate(III) is indicated by a gray line; dotted lines and gray shading represent the confidence interval.

As in the case of free hydrazones [22], all complexes under study were 1–2 orders of magnitude less cytotoxic than the standard chemotherapeutic agent doxoru-

bicin (IC_{50} = 0.18 μM for HEK293T, 95% CI [0.10; 0.33]; IC_{50} = 0.033 μM for HCT116, 95% CI [0.025; 0.042]). However, doxorubicin does not show statistically significant selectivity toward the HCT116 cell line ($p = 0.102$).

As the data in Figure 3 indicate, gold(III), in general, does not alter the cytotoxicity of hydrazones **1**–**12**. A statistically significant increase in IC_{50} in relation to the HCT116 cell line is observed for compounds **3** and **5**, while gold(III) promotes the cytotoxicity of hydrazone **6** against HCT116 and HEK293T and of hydrazone **10** against the HEK293T cell line. Tetrachloroaurate(III) itself becomes more cytotoxic for HCT116 cells upon mixing with all compounds except **3**. The differential cytotoxicity of the hydrazones alters in the presence of gold(III): among the free hydrazones, compounds **5** and **11** were more relatively selective, with IC_{50}(HEK293T)/IC_{50}(HCT116) = 8.8 and >4.8, respectively ($p < 0.001$), whereas, when mixed with gold(III), hydrazones **7** and **12** became more relatively selective (IC_{50}(HEK293T)/IC_{50}(HCT116) > 7.6 and >5.3, respectively; $p < 0.001$). The complex with compound **7** shows an IC_{50} as low as 6.6 μM, and this specific mixture can be suggested for further study in a more complicated biological model.

Limitations:

1. The equilibrium analysis described in Section 2.1 was performed in DMSO containing an aqueous titrant, whereas the cytotoxicity experiments were conducted in aqueous cell culture medium supplemented with fetal bovine serum. The chemical species present under these conditions may differ because of changes in solvent composition, pH, chloride concentration, and interactions with serum components. Furthermore, the present study did not directly monitor the oxidation state of gold or the integrity of the proposed gold(III)–hydrazone species during the 72 h incubation. Therefore, the observed biological effects cannot be attributed unambiguously to intact gold(III)–hydrazone complexes, and contributions from free ligands, other gold-containing species, or chemical transformation products cannot be excluded.
2. The cytotoxicity of the compounds was assessed using HCT116 human colorectal carcinoma cells and HEK293T transformed human embryonic kidney cells. Differences in IC_{50} values between these two cell lines indicate differential responses in the selected in vitro models. However, HEK293T cells do not constitute a normal-tissue model, and the observed differences cannot establish safety or selectivity toward normal human tissues. Further evaluation using appropriate non-transformed cells and additional biological models is necessary to assess the therapeutic potential of the compounds.

*2.3. Antimicrobial Action of Gold(III) + Hydrazones **1**–**12***

The diameters of the bacterial and fungal growth-inhibition zones (in mm) are presented in Figures 4 and S5, which represent data for both the free hydrazones and their mixtures with tetrachloroaurate(III). Representative examples of the primary experimental data (Petri dishes) are shown in Figures S6–S10.

The addition of tetrachloroaurate(III) increased the diameter of the growth-inhibition zones against *S. aureus* for most hydrazones at both tested concentrations (Figure 4). These results demonstrate an enhancement in the observed growth-inhibitory effect under the conditions of the agar well diffusion assay. However, inhibition-zone measurements alone do not distinguish pharmacological synergy from additive effects or changes in compound diffusion, solubility, or availability. Therefore, the observed enhancement cannot be classified as synergistic on the basis of the present experiments.

Inhibition of *P. aeruginosa* and *C. albicans* was also observed in the presence of tetrachloroaurate(III). The corresponding control experiments (Figures S5, S9 and S10) should be considered when interpreting these findings, because the gold-containing component may itself contribute substantially to the observed activity. The present results do not estab-

lish whether the hydrazones modify the intrinsic antimicrobial effect of gold(III), whether the components act independently, or whether specific interactions between them occur. Further quantitative combination studies are required to distinguish these possibilities.

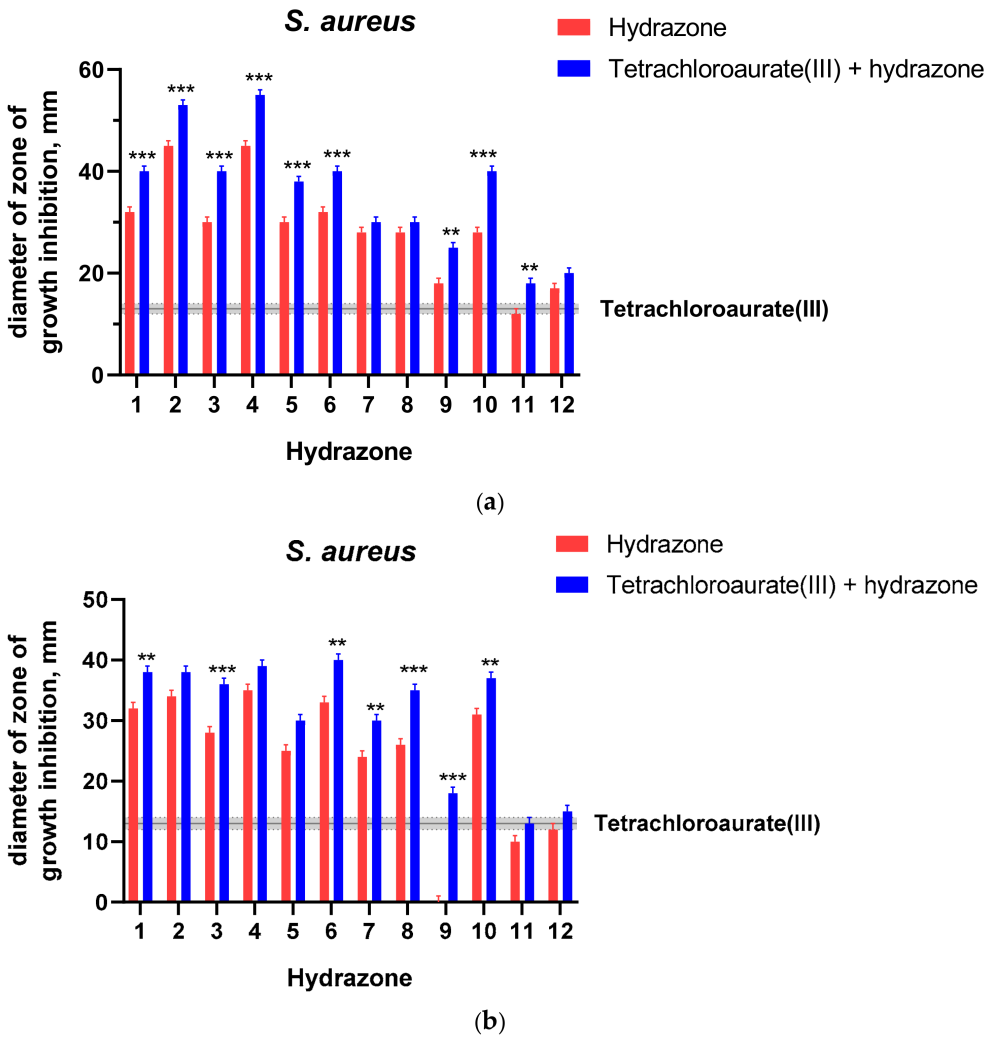


Figure 4. Diameters of growth-inhibition (mm) zones caused by free hydrazones **1**–**12** [22] and their mixtures with tetrachloroaurate(III) for S. aureus. Standard deviation of the zone diameter measurements does not exceed ±1 mm. Concentrations of hydrazone are 10 mg mL^{-1} (**a**) and 1 mg mL^{-1} (**b**), and tetrachloroaurate is taken at a concentration of 0.5 mg mL^{-1}. Asterisks denote the statistical significance level: ** $p < 0.01$, *** $p < 0.001$. The diameter of growth inhibition caused by tetrachloroaurate(III) is indicated by a gray line; dotted lines and gray shading represent the confidence interval.

The increased growth-inhibition zones observed after tetrachloroaurate(III) addition may arise from the intrinsic antimicrobial activity of the gold-containing component, changes in the physicochemical properties of the mixtures, or interactions between the components. Although membrane damage has been proposed as a mechanism for certain gold-containing antimicrobial agents [33,43], membrane integrity and compound uptake were not examined in the present study. Accordingly, membrane disruption remains a possible explanation that requires direct experimental verification.

The most pronounced promoting effect of gold(III) in relation to *S. aureus* is observed for hydrazones **2** and **4**, which were also the most prominent without metal addition. For these two compounds, the addition of gold(III), as the results of the cytotoxicity assay show (Section 2.2), does not make them more hazardous.

3. Materials and Methods

3.1. Chemicals

The synthesis of hydrazones **1**–**12** is described in the previous paper [22]. Hydrogen tetrachloroaurate(III) trihydrate, $H[AuCl_4]\cdot 3H_2O$ (Aurat, Moscow, Russia, claimed gold mass fraction 49.11%), was used without additional purification. Dimethyl sulfoxide (EKOS-1, Moscow, Russia) was also used as purchased.

3.2. Study of Gold(III) Complex Stability

An aliquot (2.53 mL) of a solution of hydrazones **1**–**12** (52–60 μM) was placed in a quartz cuvette with an optical path length of 1.00 cm and titrated with an aqueous solution of $H[AuCl_4]$ (0.01546 M). The titrant was added in 2 μL increments, and 13 to 15 data points were acquired for each experiment. All titrations were carried out in the absence of any supporting electrolyte. Pure dimethyl sulfoxide was used as a blank.

UV-Vis spectra were recorded over the wavelength range of 200 to 400 nm (absorbance range 0 to 3 log units) using a UV1800 spectrophotometer (Shimadzu, Canby, OR, USA).

All experiments were performed under ambient atmospheric pressure at a temperature of 298.2 ± 0.1 K, maintained using an external water-circulating thermostat.

3.3. Cells

The free hydrazones were not retested in the present work; their cytotoxicity values are reproduced from our earlier study [22] for comparison. The experiments reported here concern the corresponding systems containing tetrachloroaurate(III). The cell-culture and MTT procedures were based on the protocol used previously [22], with the changes in compound preparation and treatment described below.

HCT116 human colon adenocarcinoma cells and HEK293T transformed human embryonic kidney cells, both obtained from the American Type Culture Collection (ATCC), were used. The growth medium was DMEM (PanEco, Moscow, Russia) containing fetal bovine serum (10%; Cell Technologies, Shanghai, China), L-glutamine (2 mM; PanEco, Moscow, Russia), penicillin (100 U mL^{-1}; PanEco, Moscow, Russia), and streptomycin (100 μg mL^{-1}; PanEco, Moscow, Russia). Incubation was carried out at 37 °C in a humidified atmosphere with 5% CO_2.

For each hydrazone, a stock solution with a nominal concentration of 20 mM was prepared by weighing the compound on an AUW220D analytical balance (Shimadzu, Canby, OR, USA; readability 0.0005 g) and dissolving it in DMSO. The corresponding gold(III)-containing sample was prepared immediately before it was added to the cells. Stock solutions were prepared separately for each of three independent biological experiments; each biological experiment included three technical replicates.

3.4. MTT Assay

For each experiment, cells in the exponential-growth phase were dispensed into 96-well plates (3000 cells per well) and allowed to attach for 24 h before compound exposure. The tested concentration range was 0.2–50.0 μM, using successive two-fold dilutions. Doxorubicin (Veropharm, Moscow, Russia) served as the positive control. Following 72 h of treatment, 20 μL of MTT solution (5 mg mL^{-1}; PanEco, Russia) was added to each well; incubation then continued for 2–3 h. The culture medium was removed and 100 μL of DMSO was added to dissolve the resulting formazan. Absorbance was read at 570 nm with a Tecan Infinite 500 microplate reader (Tecan Group, Grodig, Austria). Viability was expressed relative to the untreated-cell control, using the ratio of absorbance in treated wells to that in control wells. Three independent biological experiments were conducted, with three technical replicates per condition in each experiment. Dose–response curves

were fitted by nonlinear regression in GraphPad Prism 8 using the mean responses, and IC_{50} values with 95% confidence intervals (CI) were obtained.

3.5. Antibacterial Assay

Antimicrobial effects were evaluated by agar well diffusion. The test panel comprised the Gram-positive strains Staphylococcus aureus ATCC 43300 and Bacillus subtilis ATCC 6633, the Gram-negative strains Escherichia coli ATCC 25922 and Pseudomonas aeruginosa ATCC 27853, and the yeast Candida albicans ATCC 14053. Before plating, each microbial suspension was adjusted to 0.5 McFarland using a DEN-1 densitometer (Bio-San, Riga, Latvia), then spread uniformly over the agar surface in Petri dishes. Mueller–Hinton agar was used for bacterial cultures; for C. albicans, the same medium was supplemented with 2% glucose. Wells 9 mm in diameter were made in the agar, and 100 μL portions of the test solutions in DMSO were added. Plates were incubated at 35 °C for 24 h, after which inhibition-zone diameters were measured. Hydrazones were assessed at 10 and 1 mg mL^{-1}. DMSO alone served as the blank control, and nifuroxazide (compound **1**) was included as a positive control.

4. Conclusions

The interaction of gold(III) with nifuroxazide and eleven related hydrazones was investigated via UV-Vis spectrophotometric titration in DMSO. The titration data were analyzed using a proposed 1:2 metal-to-ligand equilibrium model, yielding conditional formation constants with log K' values of approximately 8.8 to 9.1. Although this model provides a consistent description of the measured spectral changes, the molecular structure and coordination mode of the proposed species have not been independently established, and the possible contribution of other Au(III) species cannot be excluded.

The addition of tetrachloroaurate(III) generally produced no substantial change in the cytotoxicity of the hydrazones toward HCT116 and HEK293T cells, although compound-dependent differences were observed. These differences indicate distinct responses of the two tested cell lines but do not establish selectivity toward tumor cells relative to normal human tissue.

In agar well diffusion assays, the addition of tetrachloroaurate(III) increased the growth-inhibition zones against *S. aureus* for most hydrazones at the tested concentrations. Inhibition of *P. aeruginosa* and *C. albicans* was also observed in the presence of the gold-containing component. However, the present data do not establish pharmacological synergy or identify the molecular mechanisms responsible for these effects.

The results of this study demonstrate that the addition of tetrachloroaurate(III) can modify the observed biological activity of nifuroxazide analogs. Further studies are needed to characterize the gold-containing species, establish their stability under biological assay conditions, and quantify the effects of the individual components and their combinations. In particular, quantitative antimicrobial combination assays and additional biological models are required before the therapeutic potential of these systems can be evaluated reliably.

Because the stability and speciation of the gold-containing systems were not determined under the biological assay conditions, the observed changes in cytotoxicity and antimicrobial activity are attributed to the addition of tetrachloroaurate(III) rather than specifically to the action of structurally confirmed gold(III)–hydrazone complexes.

Supplementary Materials: The following supporting information can be downloaded at https://www.mdpi.com/article/10.3390/inorganics14110288/s1, Figure S1: Changes in UV-Vis spectra of solution of hydrazones **1**–**12** in dimethyl sulfoxide induced by aqueous $H[AuCl_4]$ addition; Figure S2: Molar extinction coefficients of free ligands and complex species formed by gold(III) and hydrazones **1**–**12** in dimethyl sulfoxide; Figure S3: Testing of different stoichiometric models of gold(III) complex

formation with hydrazone **1**: (a) ML formation; (b) ML_2 formation; Figure S4: Dose–response curves for HCT116 and HEK293T cell lines treated with tetrachloroaurate(III) mixture with hydrazones **1–12** and positive control, doxorubicin; Figure S5: Diameters of growth-inhibition (mm) zones caused by free hydrazones **1–12** and their mixtures with tetrachloroaurate(III) for *B. subtilis*, *E. coli*, *P. aeruginosa*, and *C. albicans*; Figures S6–10: Petri dishes containing *S. aureus*, *B. subtilis*, *E. coli*, *P. aeruginosa*, and *C. albicans* treated with hydrazones **1–12**. Concentrations of hydrazones **1–12** are 10 mg mL^{-1} and 1 mg mL^{-1}.

Author Contributions: Conceptualization, G.A.G. and V.S.S.; methodology, G.A.G., A.K.I. and O.N.S.; software, G.A.G.; validation, O.I.L., D.N.Y. and M.N.Z.; formal analysis, O.I.L., D.N.Y. and M.N.Z.; investigation, O.I.L., D.N.Y., A.K.I. and O.N.S.; resources, G.A.G., A.K.I. and V.S.S.; data curation, G.A.G., A.K.I. and O.N.S.; writing—original draft preparation, G.A.G. and M.N.Z.; writing—review and editing, G.A.G., A.K.I. and V.S.S.; visualization, O.N.S., A.K.I. and G.A.G.; supervision, V.S.S. and G.A.G.; project administration, G.A.G. and V.S.S.; funding acquisition, G.A.G. All authors have read and agreed to the published version of the manuscript.

Funding: This research was funded by the Russian Science Foundation, grant number 22-73-10009-P, https://rscf.ru/project/22-73-10009-P/, and a subsidy from the federal budget to higher education institutions for the implementation of activities aimed at supporting student scientific communities (V Competition of Student Scientific Communities—2026). The work of Sineva O.N. and Sadykova V.S. was carried out as part of institutional funding of the Gause Institute of New Antibiotics.

Institutional Review Board Statement: Not applicable.

Informed Consent Statement: Not applicable.

Data Availability Statement: The original contributions presented in the study are included in the article/Supplementary Material; further inquiries can be directed to the corresponding author.

Conflicts of Interest: The authors declare no conflicts of interest.

Abbreviations

The following abbreviations are used in this manuscript:

ATCC	American Type Culture Collection
CI	confidence interval
DMEM	Dulbecco's Modified Eagle's Medium
DMSO	dimethyl sulfoxide
DNA	deoxyribonucleic acid
HCT116	human colorectal carcinoma cell line
HEK293T	human embryonic kidney cell line
IC_{50}	half-maximal inhibitory concentration
MTT	3-(4,5-dimethylthiazol-2-yl)-2,5-diphenyltetrazolium bromide

References

1. Rankin, D.A.; Stahl, A.; Sabour, S.; Khan, M.A.; Armstrong, T.; Huang, J.Y.; Baggs, J.; Walters, M.S. Changes in Carbapenemase-Producing Carbapenem-Resistant Enterobacterales, 2019 to 2023. *Ann. Intern. Med.* **2025**, *178*, 1818–1821. Correction in *Ann. Intern. Med.* **2025**, *178*, 1823. https://doi.org/10.7326/ANNALS-25-04731. [CrossRef] [PubMed]
2. Devinney, K.; Burton, N.; Alroy, K.A.; Crawley, A.; Da Costa-Carter, C.-A.; Kratz, M.M.; Lin, Y.; Montfort-Gardeazabal, J.; Portier, T.; Santiago, C.; et al. *Notes from the Field*: Increase in New Delhi Metallo-β-Lactamase–Producing Carbapenem-Resistant Enterobacterales—New York City, 2019–2024. *MMWR Morb. Mortal. Wkly. Rep.* **2025**, *74*, 401–403. [CrossRef] [PubMed]
3. Marshall, J.E.; Lefrancq, N.; Mason, L.C.E.; Jawed, F.; Tam, Y.L.; Jenkins, C.; Salje, H.; Baker, K.S. The Spread of Sexually Transmissible Drug-Resistant Shigellosis in England: A Genomic Epidemiology Study. *Lancet Infect. Dis.* **2026**. [CrossRef] [PubMed]
4. Obenhuber, T.; Scheier, T.C.; Stutz, T.; Hug, M.; Fontein, D.; Kaiser, A.; Schoene, S.; Steiger, P.; Brugger, S.D.; Zingg, W.; et al. An Outbreak of Multi-Drug-Resistant Acinetobacter Baumannii on a Burns ICU and Its Control with Multi-Faceted Containment Measures. *J. Hosp. Infect.* **2024**, *146*, 102–108. [CrossRef] [PubMed]

5. Peng, W.; Hao, Y.; Ding, H.; Wang, Z.; Tan, K.; Tan, L. Root Cause Analysis for Outbreaks of Carbapenem-Resistant Acinetobacter Baumannii and Pseudomonas Aeruginosa in a Pediatric Intensive Care Unit: A Retrospective Study. *Infect. Drug Resist.* **2026**, *19*, 1–10. [CrossRef] [PubMed]
6. Staff, T. Multi-Drug-Resistant Infection Outbreak St Vincnet's Main Hospital. Available online: https://www.stvincent-times.com/multi-drug-resistant-infection-outbreak-st-vincnets-main-hospital/ (accessed on 13 August 2026).
7. Dalal, H.A.; Irfan, B.; Elmanama, A. Multidrug-Resistant Bacteria amid Health-System Collapse in Gaza. *Lancet Infect. Dis.* **2025**, *25*, 1064–1066. [CrossRef] [PubMed]
8. Alsughayer, A.; Elassar, A.-Z.A.; Hasan, A.A.; Al Sagheer, F. Antibiotic Resistance and Drug Modification: Synthesis, Characterization and Bioactivity of Newly Modified Potent Ciprofloxacin Derivatives. *Bioorganic Chem.* **2021**, *108*, 104658. [CrossRef] [PubMed]
9. Elkady, H.; Salman, I.N.; Khalifa, M.M. Small-Molecule Strategies to Combat Antibiotic Resistance: Mechanisms, Modifications, and Contemporary Approaches. *RSC Adv.* **2025**, *15*, 24450–24474. [CrossRef] [PubMed]
10. Bashimam, M.; El-Zein, H. Pharmaceutical Cocrystal of Antibiotic Drugs: A Comprehensive Review. *Heliyon* **2022**, *8*, e11872. [CrossRef] [PubMed]
11. Gomes, S.N.; Biscaia, I.F.B.; Lopes, D.S.; Mengarda, M.; Murakami, F.S.; Oliveira, P.R.; Bernardi, L.S. Cocrystals Enhance Biopharmaceutical and Antimicrobial Properties of Norfloxacin. *Pharmaceutics* **2023**, *15*, 2211. [CrossRef] [PubMed]
12. Drozd, K.V.; Manin, A.N.; Churakov, A.V.; Perlovich, G.L. Drug-Drug Cocrystals of Antituberculous 4-Aminosalicylic Acid: Screening, Crystal Structures, Thermo-chemical and Solubility Studies. *Eur. J. Pharm. Sci.* **2017**, *99*, 228–239. [CrossRef] [PubMed]
13. Drozd, K.V.; Manin, A.N.; Boycov, D.E.; Perlovich, G.L. Simultaneous Improvement of Dissolution Behavior and Oral Bioavailability of Antifungal Miconazole via Cocrystal and Salt Formation. *Pharmaceutics* **2022**, *14*, 1107. [CrossRef] [PubMed]
14. Surov, A.O.; Voronin, A.P.; Drozd, K.V.; Volkova, T.V.; Vasilev, N.; Batov, D.; Churakov, A.V.; Perlovich, G.L. Extending the Range of Nitrofurantoin Solid Forms: Effect of Molecular and Crystal Structure on Formation Thermodynamics and Physicochemical Properties. *Cryst. Growth Des.* **2022**, *22*, 2569–2586. [CrossRef]
15. Shafi, N. Metal Coordination Complexes in Antimicrobial Therapy: Advances Against Drug-Resistant Pathogens. *Microbiol. Arch. Int. J.* **2025**, *7*, 64–67. [CrossRef]
16. Sharma, B.; Shukla, S.; Rattan, R.; Fatima, M.; Goel, M.; Bhat, M.; Dutta, S.; Ranjan, R.K.; Sharma, M. Antimicrobial Agents Based on Metal Complexes: Present Situation and Future Prospects. *Int. J. Biomater.* **2022**, *2022*, 1–21. [CrossRef] [PubMed]
17. Wang, C.; Wei, X.; Zhong, L.; Chan, C.-L.; Li, H.; Sun, H. Metal-Based Approaches for the Fight against Antimicrobial Resistance: Mechanisms, Opportunities, and Challenges. *J. Am. Chem. Soc.* **2025**, *147*, 12361–12380. [CrossRef] [PubMed]
18. Tan, B.W.H.; Lee, P.F.P. Metal-Based Complexes, a Promising Solution to Antimicrobial Resistance. *Lett. Drug Des. Discov.* **2025**, *22*, 100257. [CrossRef]
19. Sharma, P.; Chaudhary, A. Green Synthesis, Coordination Properties and Emerging Applications of Schiff Base Metal Complexes: Recent Advances and Future Perspectives. *Sci. Radices* **2026**, *160*, 160–189. [CrossRef]
20. Ernest, C.M.C. Antibacterial Nitrofurfurylidene Derivatives and Methods of Using Same. U.S. Patent 3,290,213A, 12 June 1966.
21. Manin, A.N.; Drozd, K.V.; Voronin, A.P.; Churakov, A.V.; Perlovich, G.L. A Combined Experimental and Theoretical Study of Nitrofuran Antibiotics: Crystal Structures, DFT Computations, Sublimation and Solution Thermodynamics. *Molecules* **2021**, *26*, 3444. [CrossRef] [PubMed]
22. Yarullin, D.N.; Logacheva, O.I.; Isagulieva, A.K.; Sineva, O.N.; Sadykova, V.S.; Zavalishin, M.N.; Gamov, G.A. Synthesis, Cytotoxicity and Antimicrobial Action of 11 Analogs of Nifuroxazide. *Int. J. Mol. Sci.* **2026**, *27*, 7983. [CrossRef] [PubMed]
23. Odintsova, O.I.; Vladimirtseva, E.L.; Kozlova, O.V.; Smirnova, S.V.; Lipina, A.A.; Petrova, L.S.; Erzunov, K.A.; Konstantinova, Z.A.; Zimnurov, A.R.; Bykov, F.A.; et al. Finishing textile materials with microcapsules and nanoparticles of functional substances. *ChemChemTech* **2023**, *66*, 173–184. [CrossRef]
24. Rzhepishevska, O.; Hakobyan, S.; Ekstrand-Hammarström, B.; Nygren, Y.; Karlsson, T.; Bucht, A.; Elofsson, M.; Boily, J.-F.; Ramstedt, M. The Gallium(III)–Salicylidene Acylhydrazide Complex Shows Synergistic Anti-Biofilm Effect and Inhibits Toxin Production by Pseudomonas Aeruginosa. *J. Inorg. Biochem.* **2014**, *138*, 1–8. [CrossRef] [PubMed]
25. Ratia, C.; Sueiro, S.; Soengas, R.G.; Iglesias, M.J.; López-Ortiz, F.; Soto, S.M. Gold(III) Complexes Activity against Multidrug-Resistant Bacteria of Veterinary Significance. *Antibiotics* **2022**, *11*, 1728. [CrossRef] [PubMed]
26. Ratia, C.; Ballén, V.; Gabasa, Y.; Soengas, R.G.; Velasco-de Andrés, M.; Iglesias, M.J.; Cheng, Q.; Lozano, F.; Arnér, E.S.J.; López-Ortiz, F.; et al. Novel Gold(III)-Dithiocarbamate Complex Targeting Bacterial Thioredoxin Reductase: Antimicrobial Activity, Synergy, Toxicity, and Mechanistic Insights. *Front. Microbiol.* **2023**, *14*, 1198473. [CrossRef] [PubMed]
27. Mansour, A.M. Synthesis, Spectroscopic, Electrochemical, DFT and SAR Studies of Nifuroxazide Complexes with Pd(II), Pt(II) and Ru(II). *Polyhedron* **2014**, *78*, 10–17. [CrossRef]
28. Mansour, A.M. Influence of Metal Complex Formation on the Antimicrobial Activity of Nifuroxazide: Spectroscopic, Electrochemical, and DFT Studies. *J. Coord. Chem.* **2016**, *69*, 215–226. [CrossRef]

29. Abd El-Lateef, H.M.; El-Taib Heakal, F.; Khalaf, M.M.; Abdou, A. Synthesis, and Characterization of Mn(II), VO(II), and Cu(II) Complexes of Nifuroxazide and Salicylic Acid: A Study of Structural Features, DFT Calculations, Molecular Docking, and Biological Activities. *J. Indian Chem. Soc.* **2026**, *103*, 102388. [CrossRef]
30. Radisavljević, S.; Petrović, B. Gold(III) Complexes: An Overview on Their Kinetics, Interactions With DNA/BSA, Cytotoxic Activity, and Computational Calculations. *Front. Chem.* **2020**, *8*, 379. [CrossRef] [PubMed]
31. Büssing, R.; Karge, B.; Lippmann, P.; Jones, P.G.; Brönstrup, M.; Ott, I. Gold(I) and Gold(III) N-Heterocyclic Carbene Complexes as Antibacterial Agents and Inhibitors of Bacterial Thioredoxin Reductase. *ChemMedChem* **2021**, *16*, 3402–3409. [CrossRef] [PubMed]
32. Ratia, C.; Soengas, R.G.; Soto, S.M. Gold-Derived Molecules as New Antimicrobial Agents. *Front. Microbiol.* **2022**, *13*, 846959. [CrossRef] [PubMed]
33. Ratia, C.; Cepas, V.; Soengas, R.; Navarro, Y.; Velasco-de Andrés, M.; Iglesias, M.J.; Lozano, F.; López-Ortiz, F.; Soto, S.M. A C∧S-Cyclometallated Gold(III) Complex as a Novel Antibacterial Candidate Against Drug-Resistant Bacteria. *Front. Microbiol.* **2022**, *13*, 815622. [CrossRef] [PubMed]
34. Wróblewska, A.; Sadowski, M.; Jasiński, R. Selectivity and Molecular Mechanism of the Au(III)-Catalyzed [3+2] Cycloaddition Reaction between (Z)-C,N-Diphenylnitrone and Nitroethene in the Light of the Molecular Electron Density Theory Computational Study. *Chem. Heterocycl. Compd.* **2024**, *60*, 639–645. [CrossRef]
35. Sékou, D.; Bamba, F.; Affoué Lucie, B.; Gbèdodé Wilfried, K.; Assongba Gaston, K.; El-Hadji Sawaliho, B. Study by Quantum Chemical of Relationship between Electronic Structure and SecA Inhibitory Activity of a Series 5-Cyano Thiouracil Derivatives. *J. Mater. Phys. Chem.* **2022**, *10*, 43–48. [CrossRef]
36. Doyle, A.A.; Krämer, T.; Kavanagh, K.; Stephens, J.C. Cinnamaldehydes: Synthesis, Antibacterial Evaluation, and the Effect of Molecular Structure on Antibacterial Activity. *Results Chem.* **2019**, *1*, 100013. Correction in *Results Chem.* **2020**, *2*, 100050. https://doi.org/10.1016/j.rechem.2020.100050. [CrossRef]
37. Shaw, C.F. Gold-Based Therapeutic Agents. *Chem. Rev.* **1999**, *99*, 2589–2600. [CrossRef] [PubMed]
38. Gamov, G.A. Complexation of Gold(I) and Gold(III) in Solutions. *Coord. Chem. Rev.* **2024**, *520*, 216162. [CrossRef]
39. Meshkov, A.N.; Gamov, G.A. KEV: A Free Software for Calculating the Equilibrium Composition and Determining the Equilibrium Con-stants Using UV–Vis and Potentiometric Data. *Talanta* **2019**, *198*, 200–205. [CrossRef] [PubMed]
40. Kuranova, N.N.; Pimenov, O.A.; Zavalishin, M.N.; Gamov, G.A. Complexes of Gold(III) with Hydrazones Derived from Pyridoxal: Stability, Structure, and Nature of UV-Vis Spectra. *Int. J. Mol. Sci.* **2024**, *25*, 5046. [CrossRef] [PubMed]
41. Khan, M.A.; Kauser Ali, S.; Bouet, G.M. Solvent Effects on the Stability of Nifuroxazide Complexes with Cobalt(II), Nickel(II) and Copper(II) in Alcohols. *J. Inorg. Biochem.* **2002**, *90*, 67–70. [CrossRef] [PubMed]
42. Logacheva, O.I.; Pimenov, O.A.; Gamov, G.A. UV–Vis Spectra of Gold(III) Complexes with Different Halides, Hydroxide, and Ammonia According to TD-DFT Calculations. *Chemistry* **2025**, *8*, 3. [CrossRef]
43. Paesa, M.; Remirez De Ganuza, C.; Alejo, T.; Yus, C.; Irusta, S.; Arruebo, M.; Sebastian, V.; Mendoza, G. Elucidating the Mechanisms of Action of Antibiotic-like Ionic Gold and Biogenic Gold Nanoparticles against Bacteria. *J. Colloid Interface Sci.* **2023**, *633*, 786–799. [CrossRef] [PubMed]

Disclaimer/Publisher's Note: The statements, opinions and data contained in all publications are solely those of the individual author(s) and contributor(s) and not of MDPI and/or the editor(s). MDPI and/or the editor(s) disclaim responsibility for any injury to people or property resulting from any ideas, methods, instructions or products referred to in the content.